Biogeosciences, 23, 4515–4527, 2026
https://doi.org/10.5194/bg-23-4515-2026

Biogeosciences Open Access EGU

Ocean acidification alters phytoplankton diversity and community structure in the coastal water of the East China Sea

Yuming Rao[1,★], Na Wang[2,★], He Li[3], Jiazhen Sun[2], Xiaowen Jiang[2], Di Zhang[2], Liming Qu[2], Qianqian Fu[2], Xuyang Wang[2], Cong Zhou[2], Zichao Deng[2], Yang Tian[2], Xiangqi Yi[2], Ruiping Huang[2], Guang Gao[2], Xin Lin[2], and Kunshan Gao[1,3]

[1]State Key Laboratory of Marine Environmental Science, College of the Environment and Ecology, Xiamen University, Xiamen, China
[2]State Key Laboratory of Marine Environmental Science, College of Ocean and Earth Science, Xiamen University, Xiamen, China
[3]Co-Innovation Center of Jiangsu Marine Bio-industry Technology, Jiangsu Ocean University, Lianyungang 222005, China
★These authors contributed equally to this work.

Correspondence: Kunshan Gao (ksgao@xmu.edu.cn)

Received: 21 October 2025 – Discussion started: 24 November 2025
Revised: 4 June 2026 – Accepted: 12 June 2026 – Published: 6 July 2026

Abstract. Anthropogenic CO_2 emissions and their continuous dissolution into seawater lead to seawater pCO_2 rise and ocean acidification (OA). Phytoplankton groups are known to be differentially affected by carbonate chemistry changes associated with OA in different regions of contrasting physical and chemical features. To explore responses of phytoplankton to OA in the Chinese coastal waters, we conducted a mesocosm experiment in a eutrophic bay of the southern East China Sea under ambient (410 µatm, AC) and elevated (1000 µatm, HC) pCO_2 levels. The HC condition stimulated phytoplankton growth and primary production during the initial nutrient-replete stage, while the community diversity and evenness in both pCO_2 treatments were reduced during this stage due to the rapid nutrient consumption and diatom blooms, and the subsequent shift from diatoms to heterodinoflagellates led to a decline in primary production during the mid and later phases under nutrient depletion. HC treatment suppressed the diatom-to-dinoflagellate succession and enhanced the subsequent remineralization of organic matter, thereby facilitating smaller phytoplankton to dominant and sustaining primary production. Our findings indicate that, the impacts of OA on phytoplankton diversity in the coastal water of the southern East China Sea depend on availability of nutrients, with primary productivity and biodiversity of phytoplankton reduced in the eutrophicated coastal water.

1 Introduction

It is commonly known that sequestration of CO_2 in coastal waters play important roles against global warming due to their high primary productivity (Rogelj et al., 2022), which resulted in faster CO_2 removal due to photosynthesis than dissolution of CO_2 from the air (Stukel et al., 2023). It has been assessed that, with the increasing anthropogenic CO_2 emissions, the oceanic CO_2 sink increased from $1.7 \pm 0.4\,\mathrm{pg\,C\,yr^{-1}}$ in the 1980s to $2.5 \pm 0.6\,\mathrm{pg\,C\,yr^{-1}}$ in the 2010s (Friedlingstein et al., 2025). Nevertheless, such apparent oceanic CO_2 uptake is altering carbonate chemistry in surface oceans, leading to a pH drop of by 0.017–0.027 units per decade, with a potential further drop by 0.3–0.4 units at the end of this century (Canadell et al., 2023; Gattuso et al., 2015). Such progressive ocean acidification (OA) has been shown to impact many marine organisms (Gattuso et al., 2015), including primary producers (Gao et al., 2020), subsequently feeding back on the CO_2 sequestration efficiency in marine systems including coastal waters.

OA in eutrophic coastal waters are suggested to progress faster than in open oceans by roughly 20 % due to CO_2 dissolution and enhanced remineralization of organic maters (Cai et al., 2011). The subsequent changes in carbonate chemistry may thus drive shifts in phytoplankton community structures/diversity and affect primary productions in

differential ways due to regional environmental traits and species-specific physiology (Feng et al., 2024; Gao et al., 2012). While the effects of elevated pCO_2 on different phytoplankton assemblages have been demonstrated, positive, neutral and negative effects have been reported, reflecting differences in experimental approaches and/or phytoplankton compositions (Gao et al., 2020). Among the different approaches, field mesocosm experiments under elevated pCO_2 projected for future OA scenario have been employed to investigate the effects of OA on ecological processes, including primary production. For example, mesocosm experiments showed that growth of coccolithophores was reduced under 710 µatm pCO_2 during early summer in 2001 (Engel et al., 2005) and their ability to form blooms disappeared under 1000–3000 µatm pCO_2 during early summer in 2011 (Riebesell et al., 2017). Under elevated pCO_2, phytoplankton communities in Norwegian coastal mesocosms shifted from *Bathycoccus* to *Micromonas* (Meakin and Wyman, 2011). In oligotrophic or mesotrophic conditions, diatoms were insensitive to OA but responded positively under nutrient enrichment (Bach et al., 2019). Furthermore, nutrients enrichment also increased Chl *a* concentration under high pCO_2 condition (Riebesell et al., 2017; Tanaka et al., 2013; Schulz et al., 2013). By contrast, mesocosm experiments conducted in highly eutrophic water showed that high pCO_2 did not affect Chl *a* concentration (Liu et al., 2017). Previously, we showed, by running a mesocosm experiment during spring of 2018 in the southern coastal water of the East China Sea, that elevated pCO_2 of 1000 µatm suppressed the succession from diatoms to dinoflagellates and increased the abundance of viruses and heterotrophic bacteria, promoting refueling of nutrients for phytoplankton growth (Huang et al., 2021). These findings indicate that plankton communities supported by nutrients from remineralization are more sensitive to OA than those having access to higher availability of inorganic nutrients (Bach et al., 2016, 2019). Overall, it is likely that the effects of OA on community structure can vary temporally and spatially, and the availabilities or levels of eutrophication can modulate the effects of OA, alongside regional chemical and physical differences (Paul and Bach, 2020).

In coastal regions, changes in seawater carbonate chemistry influence primary production which in reverse affect the pH change due to faster photosynthetic CO_2 removal than its dissolution (Gao, 2021), resulting in increased pH during daytime and declined pH during nighttime. Such large diel pH fluctuation may require phytoplankton to invest more energy to maintain cellular homeostasis in response to the negative effects of increased hydrogen ion concentration (the acidic stress), thereby affecting the functioning of planktonic ecosystem (Raven and Beardall, 2020; Rokitta et al., 2012; Taylor et al., 2017). The positive effects of increased inorganic carbon substrates (e.g., CO_2 and HCO_3^-) and the negative effect of increased H^+ concentration may shape the responses of coastal ecosystems to OA, leading to controversial results (Wu et al., 2017; Vázquez et al., 2023; Chauhan et al., 2024). To better understand the consequences of OA in Chinese eutrophic coastal regions, we conducted a mesocosm experiment in the eutrophic coastal water of Wuyuan Bay, Xiamen, China, using in situ plankton communities during October–December, 2019 and investigated how OA shapes the diversity of phytoplankton community and affects primary production processes. Our results show that in the eutrophic coastal water of East China Sea, with the natural decrease of temperature, elevated pCO_2 increased primary production by promoting the phytoplankton biomass (indicated by Chl *a* concentration) under nutrient-replete condition, and promoted smaller phytoplankton's growth to sustain the primary production after the nutrient depletion and diatom bloom collapsed, though suppressed the emergence of dinoflagellates.

2 Materials and methods

2.1 Mesocosms setup and sampling

The in situ mesocosm experiment was conducted at the Facility for the Study of Ocean Acidification Impacts of Xiamen University (FOANIC-XMU) located in the subtropical coastal region Wuyuan Bay of southern East China Sea (24.52° N, 117.18° E) from 9 October (day 0 relative to algal inoculation) to 14 November, 2019. Nine cylindrical and transparent thermoplastic polyurethane (TPU) mesocosm bags, each 3 m deep and 1.5 m in diameter, were filled with approximately 3000 L of in situ seawater that had been prefiltered (MU801-4T, Midea, China, pore size of 0.01 µm). The mesocosms were hooked to and secured within steel frames. Two pCO_2 treatments were established to investigate the effects of ocean acidification on the in situ phytoplankton community: an ambient pCO_2 treatment (AC, 410 µatm; 4 numbered bags) and a high pCO_2 treatment representative of end-of-century projections (HC, 1000 µatm; 5 numbered bags). To adjust CO_2 in seawater in the HC bags to the projected 1000 µatm in 2100s, approximately 11 L of CO_2-saturated seawater was added to each HC bag. The AC and HC pCO_2 levels were maintained by bubbling with ambient air and pre-mixed air-CO_2 (1000 µatm CO_2), respectively, at a rate of 5 L min^{-1} using a CO_2 Enricher (CE-100B, Wuhan Ruihua Instrument & Equipment Ltd, China). After the carbonate system had been stabilized (leveled pH), 720 L of in situ seawater were filtered by a 180 µm mash to exclude large zooplankton, and each mesocosm bag was inoculated with 80 L of it to initiate the coastal microbial community. Samples were taken from each bag at a depth of 0.5 m at 9:00 a.m. by niskin bottles every 1–3 d for physical, chemical and biological analysis.

2.2 Measurement of environmental factors

Solar light intensity was monitored every minute throughout the experimental period using a real-time solar irradiance

monitoring device (EKO, Japan). Salinity, temperature and pH in each mesocosm were measured with a salinometer, a digital thermometer and a pH meter (Orino 2 STAR, Thermo Scientific, USA, calibrated with standard NBS buffer), respectively. Dissolved inorganic carbon (DIC) was sampled and measured using an Environmental Water Analyzer (Ma et al., 2018), and total alkalinity (TA) measured using an Automated Spectrophotometric Analyzer (Li et al., 2013). Other seawater carbonate chemistry parameters were calculated with CO2SYS software with known parameters of pCO_2, salinity, pH, temperature, and nutrient concentration.

Nutrient samples of each bag were filtered through cellulose acetate membrane (0.22 µm, 47 mm), and the filtrate was divided into 2 subsamples; one was stored at −20 °C for the measurement of $NO_3^- + NO_2^-$, PO_4^{3-}, and NH_4^+; another stored at 4 °C for the measurement of SiO_3^{2-}. Measurement of $NO_3^- + NO_2^-$, PO_4^{3-}, and SiO_3^{2-} concentration was conducted using an auto-analyzer (AA3, Seal, Germany), NH_4^+ was measured with indophenol blue spectrophotometry using a spectrophotometer (Tri-223, Spectrum, China) at 25 °C. NO_2^- and NO_3^- were analyzed using the copper-cadmium reduction method, the standard concentrations used for the $NO_2^- + NO_3^-$ calibration curve were 0, 1.04, 2.08, 4.16, 10.4, 20.8, and 41.6 µM, and those for NO_2^- calibration curve were 0, 0.04, 0.08, 0.16, 0.4, 0.8, and 1.6 µM (Dai et al., 2008). PO_4^{3-} and SiO_3^{2-} were measured using typical spectrophotometric method (Intergovernmental Oceanographic Commission, 1994), and the calibration curves of both parameters were prepared using standard concentrations of 0, 0.08, 0.16, 0.32, 0.8, 1.6, 3.2 µM and 0, 4, 8, 16, 40, 80, 160 µM, respectively.

2.3 Measurement of Chlorophyll *a* and particle organic matters

Water samples of each mesocosm (100–1000 mL, depending on the biomass in the mesocosms) were filtered onto GF/F filter (Whatman, United States) by suction filter with low vacuum pressure (< 0.02 Mpa) and soaked in 5 mL pure methanol overnight. The extracts were centrifuged at 8000 × *g* and 4 °C for 10 min, then the absorption spectra of supernatants from 400 to 800 nm were measured using a UV-VIS spectrophotometer (DU 800, Beckman, USA). The Chl *a* concentration was calculated according to the following equation (Ritchie, 2006):

$$\text{Chl } a(\mu g\,L^{-1}) = 16.29 \times (A665 - A750) - 8.54 \times (A652 - A750)$$

where *A*750, *A*665, and *A*652 represents the absorbance of Chl *a* at wave length 750, 665, and 652 nm, respectively.

For the analysis of particulate organic carbon (POC) and nitrogen (PON) across two particle size fractions, water samples of known volume were first filtered through a 20 µm mash to obtain subsamples containing particle organic matters smaller than 20 µm. Particles larger than 20 µm (retained on 20 µm mesh) were backwashed using an equal volume of prefiltered (0.22 µm) in situ seawater, yielding in subsamples containing particulate organic matters larger than 20 µm. All subsamples were then filtered on precombusted (450 °C, 6 h) GF/F filter (Whatman) and stored at −20 °C until analysis. Before analyses, all filters were fumed over pure HCl for 12 h and dried at 60 °C to remove inorganic carbon, then packed in tin cups and measured with a CHNS elemental analyzer (Vario EL cube Elementar, Germany).

2.4 Net primary production and dark respiration

Before sunrise, 120 mL of water samples from each mesocosm were collected and dispensed into six 25 mL borosilicate bottles (three bottles for 12 h incubations, and three for 24 h incubations). For each culture duration of each mesocosm, two bottles were illuminated under natural light and one bottle was wrapped tightly in aluminum foil as a dark control. After incubation, cells were filtered onto the GF/F filters (Whatman) under dim light and stored at −20 °C. Before measurement, filters were placed individually in 20 mL scintillation vials and exposed to HCl fumes overnight, dried at 60 °C for over 6 h to remove any unincorporated $H^{14}CO_3^-$. The incorporated ^{14}C by algae was counted with a liquid scintillation counter (Beckman, LS6500, Germany) in the presence of 5 mL scintillation cocktail (Hisafe 3, Perkin-Elmer, United States). Nighttime respiratory carbon loss was calculated as the difference between carbon fixation over 12 h (daytime primary production) and 24 h (daily net primary production).

2.5 Determination of phytoplankton biomass and community structure

Water samples (500–2000 mL) from each mesocosm were collected into polyethylene bottles and fixed with 1.5 % acidic lugol's iodine. The samples were statically placed for 2–3 d and concentrated into 50 mL subsamples in the centrifuge tube using siphons within 3 d, then examined with a microscopy (Nikon Eclipse Ns2) and a plankton counting chamber to assess phytoplankton abundance and diversity based on the morphological characteristics as previous described (Hasle and Syvertsen, 1997; Steidinger and Jangen, 1997; Yang and Liu, 2018). To distinguish whether dinoflagellates are autotrophic or heterotrophic, we observed living algal cells in the unstained water samples under the microscope for cell transparency and the presence of chloroplasts.

An aliquot of 100 µL for each mesocosm was loaded onto a counting chamber for microscopic enumeration. In each aliquot, the count was deemed valid only when the total number of cells exceeded 200; otherwise, the subsample volume for microscopy was increased to achieve sufficient

counts. For samples collected during the exponential growth phase that exhibited excessively high cell densities, appropriate dilution with 0.22 µm-filtered, sterilized seawater was performed prior to counting (State Oceanic Administration, 2005).

2.6 Statistical analyses

The data were all expressed by the mean and standard deviation (means ± SD) and plotted by Origin 2024. Independent-samples t test was conducted to check the significant effects of increased pCO_2 at the level of $p < 0.05$ using SPSS 19. To evaluate α-diversity, Shannon diversity index was calculated based on the relative abundances of phytoplankton taxa using the estimate R and diversity functions from the vegan package (version 2.6-4) in R (Version 4.2.2). Shannon index incorporates both species diversity and evenness. Patterns of physiological parameters over time were emphasizing using generalized additive models (GAMs) and constructed using the 'mgcv' package in R to analyze changes in physiology through the experiment.

3 Results

3.1 Environmental changes in the mesocosms

Throughout the experiment, most days were sunny, with daytime mean PAR (12 h-average photosynthetic active radiation) ranging from 200 to 850 µmol photons $m^{-2}\,s^{-1}$ (Fig. S1 in the Supplement). The environmental temperatures decreased gradually from 26.7 ± 0.05 °C at day 0 (9 October) to 21.1 ± 0.28 °C at day 38 (14 November) (Fig. 1a). Significant differences in pH_{NBS} and pCO_2 between HC and AC were maintained throughout most of the experimental period, while there's no significant difference in total alkalinity (TA) between the two pCO_2 treatments ($p = 4.02 \times 10^{-8}$, 2.87×10^{-12}, 0.549, respectively. Figures 1b–d and S5a–c).

Following a sharp increase in phytoplankton biomass from day 4 to day 8 (Fig. 3a), the pH_{NBS} in the HC and AC mesocosms increased and peaked at 8.24 ± 0.16 and 8.56 ± 0.14, respectively (Fig. 1b). Correspondingly, the pCO_2 value dropped to the lowest points of 238.48 ± 49.02 µatm (HC) and 82.82 ± 32.88 µatm (AC) (Fig. 1c). Then, as the phytoplankton biomass decreased after day 8, pH_{NBS} gradually declined and pCO_2 increased, both stabilizing at relatively constant levels from day 18 until the end of experiment. There were no obvious temporal changes observed in total alkalinity (TA) throughout the experiment (Fig. 1d).

The initial nutrient concentrations reflected the eutrophic condition in the coastal seawater ($NO_3^- + NO_2^-$: 27 µM, PO_4^{3-}: 1.4 µM). In the mesocosm bags, nutrient concentrations declined dramatically in the early phase (up to day 8, Fig. 2). The $NO_3^- + NO_2^-$ and NO_3^- concentrations decreased sharply to nearly 0 by day 8 (Fig. 2a and b). In contrast,

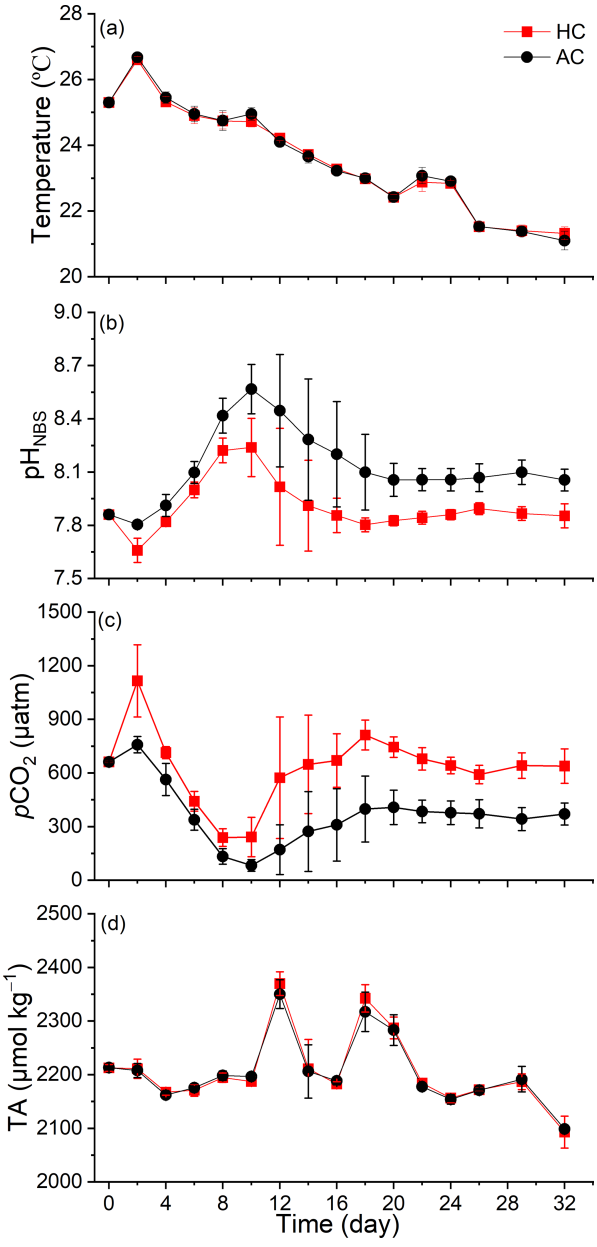

Figure 1. Temporal variation of seawater temperature **(a)**, pH_{NBS} **(b)**, pCO_2 **(c)** and TA **(d)** in HC (1000 µatm) and AC (410 µatm) mesocosms. The pCO_2 was estimated from the measured pH_{NBS} and DIC concentration using the CO2SYS program. Data are means ± SD of 5 replicates for HC and 4 replicates for AC mesocosms.

the NO_2^- concentration experienced a slight increase on day 2, then declined to nearly 0 by day 8 and remained at a low level until the end of experiment in both HC and AC mesocosms (Fig. 2c). Under HC condition, the NO_3^- concentration decreased more rapidly than that under the AC until day 20, although the difference was not significant ($p = 0.423$, Fig. S5d). Both NH_4^+ and PO_4^{3-} concentrations dropped to nearly 0 after 4 d and remain relatively sta-

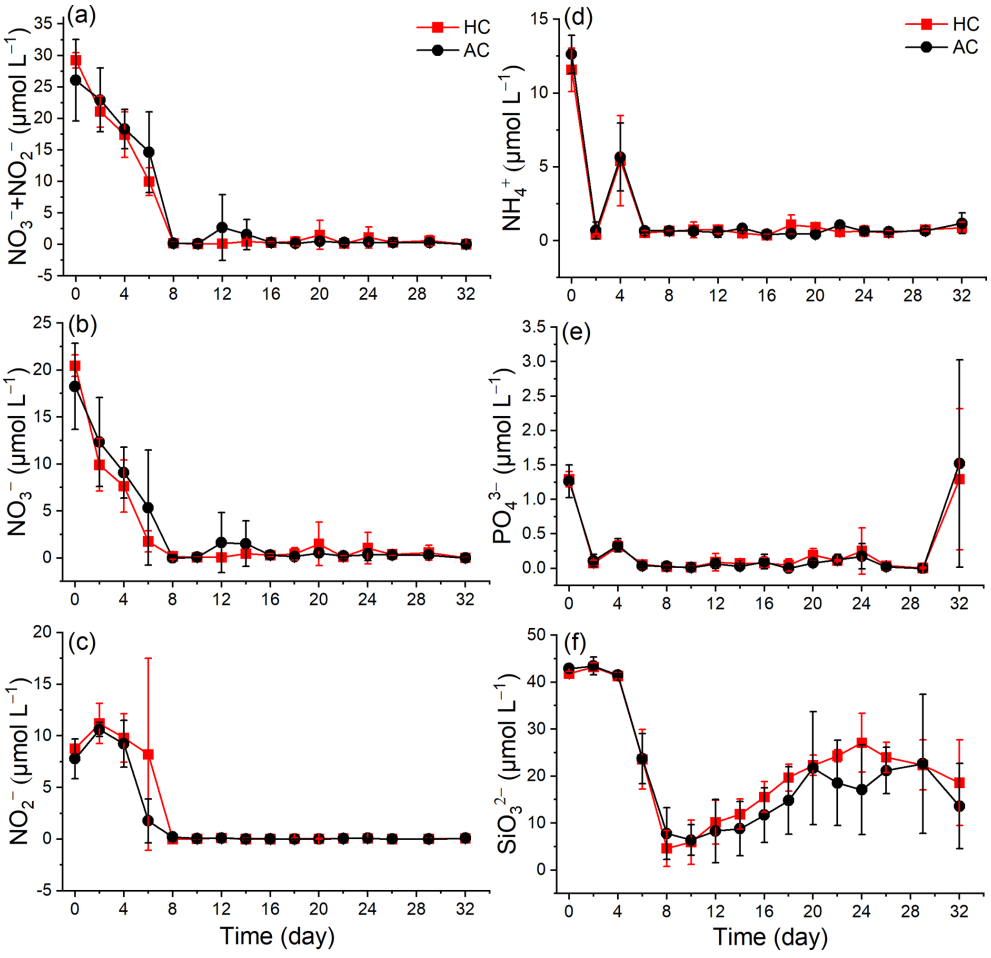

Figure 2. Temporal variation of nutrients (NO_3^-, NO_2^-, $NO_3^- + NO_2^-$, NH_4^+, PO_4^{3-}, and SiO_3^{2-}) in HC (1000 µatm) and AC (410 µatm) mesocosms. Data are means ± SD of 5 replicates for HC and 4 replicates for AC mesocosms.

ble thereafter. There were no significant difference observed between HC and AC mesocosms ($p = 0.579$ and 0.631, respectively, Figs. 2d, e and S5e, f). The SiO_3^{2-} concentration decreased from 41.81 ± 0.48 µM in HC and 42.88 ± 0.91 µM in AC on day 0 to a minimum of 4.62 ± 3.82 µM and 7.79 ± 5.52 µM by day 8, respectively. Thereafter, SiO_3^{2-} concentrations in both HC and AC mesocosms gradually increased until the end of experiment ($p = 0.343$, Figs. 2f and S5g).

3.2 Chlorophyll *a* concentration

Phytoplankton biomass, indirectly indicated by Chl *a* concentration, increased to peak at 35.88 ± 3.25 µg L^{-1} in the HC and 36.54 ± 4.88 µg L^{-1} in the AC mesocosms on day 8, and then gradually decreased to 1.12 ± 0.43 µg L^{-1} in HC by day 14 and 0.58 ± 0.31 µg L^{-1} in AC by day 16, followed by a slight increase by the end of experiment (Fig. 3a). Based on the natural logarithm (ln) scale of Chl *a* concentration, the phytoplankton growth kinetics under the two pCO_2 treatments showed the following phases (Fig. 3b): the exponential phase (from day 0 to day 5), the stationary phase (from day 6 to day 10), the decline phase (from day 11 to day 16), and a second exponential phase from day 17 to day 24 in the HC and to day 20 in the AC mesocosms. Then, phytoplankton assemblages in the HC mesocosms entered a second stationary phase until the end of experiment, while in the AC ones, they entered a decline phase until day 29, followed by a slight increase on day 32.

Throughout the experiment, the elevated pCO_2 resulted in higher average value of Chl *a* concentration at most sampling times, although the differences were not statistically significant ($p = 0.142$, Fig. S5h).

3.3 Primary production and dark respiration

The primary production and night-respiratory per water volume showed patterns similar to those of phytoplankton biomass (indicated by Chl *a* concentration) (Fig. 4a–c). They reached their maximal values on day 6, which corresponded to the end of exponential phase. As the phytoplankton communities entered the stationary phase, daytime (12 h) primary

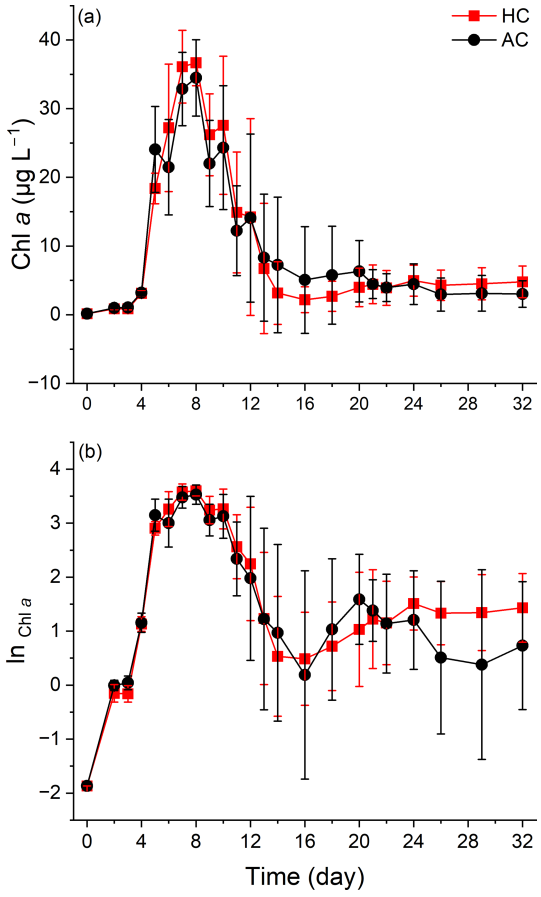

Figure 3. Temporal variations of Chl *a* concentration **(a)** and the LN scale of Chl *a* concentration **(b)** in HC (1000 µatm) and AC (410 µatm) mesocosms. Data are means ± SD of 5 replicates for HC and 4 replicates for AC mesocosms.

production, daily (24 h) net primary production and nighttime respiration per water volume progressively decreased, and then slightly increased again when the phytoplankton communities underwent the second exponential phase. The elevated pCO_2 increased both daytime and daily net primary production during the middle phase of the experiment, although the positive effect on 24 h primary production tended to decline by the end of experiment ($p = 0.038$ and 0.012, Fig. S6a and b). The nighttime respiration of phytoplankton was suppressed before day 8 and enhanced thereafter under the elevated pCO_2, though no significant difference was observed ($p = 0.444$, Fig. S6c).

Primary productivity per Chl *a* increased sharply on day 4, and decreased to the lowest values on day 8. On day 12, both daytime and 24 h primary productivity in the HC increased drastically and then remained relatively stable until the end of experiment (Fig. 4d and e). In contrast, two additional peaks were observed in the AC mosocosms on days 16 and 26. The elevated pCO_2 appeared to have enhanced primary productivity from day 2 to day 20, though these effects were not statistically significant ($p = 0.946$ for daytime and $p = 0.985$ for 24 h, Figs. 4d, e and S6d, e).

Nighttime respiration per µg Chl *a* initially increased on day 4, then decreased to nearly zero in both the HC and AC mesocosms on day 8 and remained relatively stable till the end of experiment. The elevated pCO_2 had a negative effect on phytoplankton respiration before day 12, but increased it thereafter, though no significant difference was observed between the HC and AC treatments ($p = 0.834$, Figs. 4f and S6f).

3.4 Changes in Phytoplankton community and diversity

A total of 47 genera identified microscopically include 33 genera of diatoms, 7 of dinoflagellates, 2 of cyanobacteria, 2 of chlorophyta, 2 of cryptophyta and 1 of euglenophyta. In all mesocosms, the dominant species included *Cerataulina pelagica*, *Eucampia cornuta*, *Guinardia delicatula*, *Leptocylindrus danicus*, *Skeletonema costatum*, *Protoperidinium* sp., *Gyrodinium spirale*, *Cryptophyta* sp. and *Pyramimonas* sp. (Fig. S4).

Phytoplankton communities underwent dynamic succession in the mesocosms (Fig. 5). Diatoms (mainly *Cerataulina pelagica*) dominated the phytoplankton communities during the early and middle stages of the experiment, as indicated by the similar temporal trends in total phytoplankton and diatom cell counts compared with Chl *a* concentration (Figs. 5a, b and S4a). There was no significant difference in diatom density between the HC and AC mesocosms ($p = 0.259$, Fig. S7a), although the average value was lower in the former than in the latter treatment. Autotrophic dinoflagellates began to emerge on day 8 and rapidly declined on day 12 in both HC and AC enclosures (Fig. 5c). Except for days 6 to 18, the elevated pCO_2 increased the biomass of autotrophic dinoflagellates, though the difference was insignificant ($p = 0.505$, Fig. S7b). Hetero-dinoflagellates began to emerge on day 6, with their abundance peaked on day 12 in the AC and on day 14 in the HC mesocosms, then decreased by day 22. The elevated pCO_2 did not result in any significant change in terms of their cell numbers ($p = 0.785$, Figs. 5d and S7c). On day 26, the biomass of hetero-dinoflagellates increased again in the HC treatment, while it remained constant in the AC treatment ($p = 0.729$, Independent-samples *t* test).

The biomass of small taxa (Cyanobacteria, Chlorophyta, Cryptophyta and Euglenophyta) started to increase on day 8, the HC treatment significantly increased the total biomass of these small phytoplankton species thereafter ($p = 0.019$, Figs. 5e, S4h, i and S7d). From day 22, when diatoms biomass decreased to the lowest level, the temporal variation in small taxa biomass became the main factor controlling overall phytoplankton dynamics (Fig. 5e and S4h, i). Accordingly, the positive effect of HC on the small phytoplankton species led to an earlier transition of phytoplank-

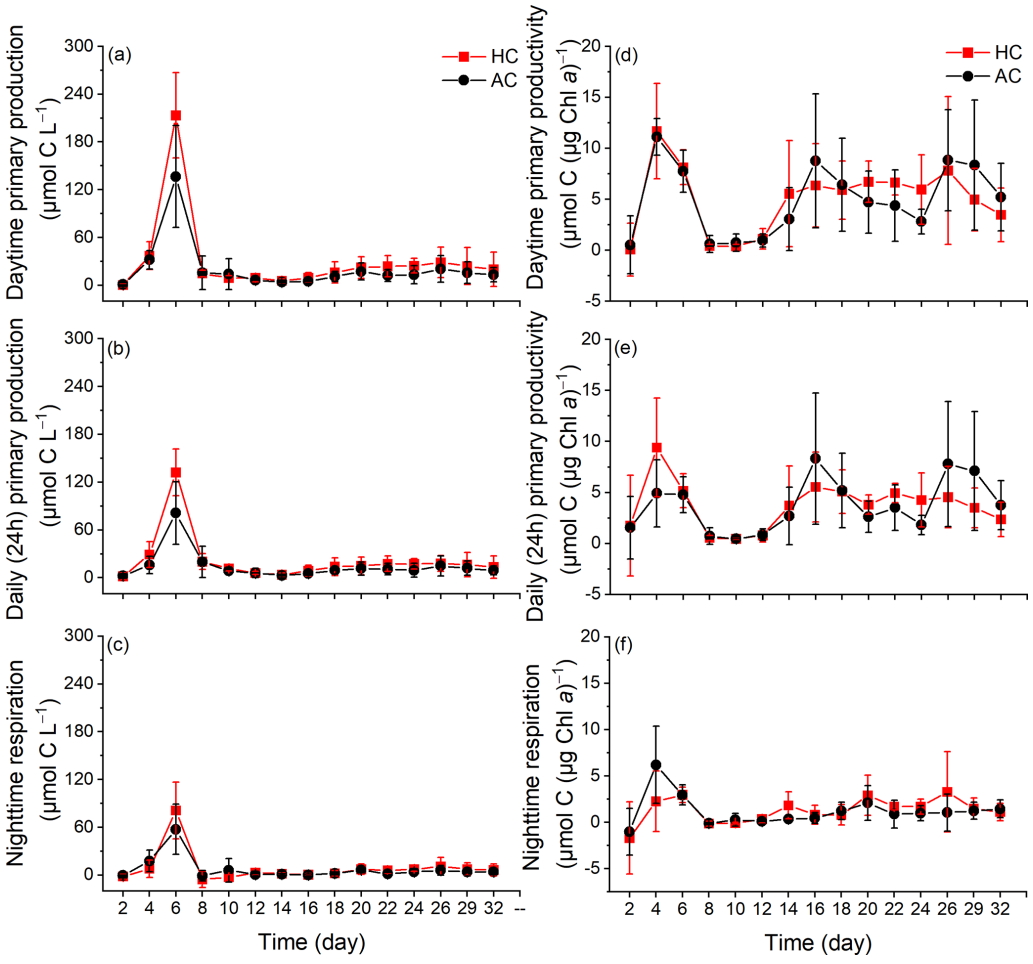

Figure 4. The changes of daytime primary production **(a)** and primary productivity **(b)**, daily (24 h) primary production **(c)** and primary productivity **(d)**, nighttime respiration per water volume **(e)** and per Chl *a* **(f)** in HC (1000 µatm) and AC (410 µatm) mesocosms. Data are means ± SD of 5 replicates for HC and 4 replicates for AC mesocosms.

ton from the large diatoms and dinoflagellate (mainly fall within the micro size fraction) to the smaller ones (Fig. 6a and b). This accelerated transition in the HC treatment was also evidenced by higher concentration of POC and PON in the < 20 µm fraction and lower concentration in the > 20 µm fraction (Figs. S2 and S3).

In both HC and AC mesocosms, Shannon diversity index decreased sharply from day 2, reaching the lowest values on day 8 in AC mesocosms and on day 10 in HC mesocosms (Fig. S8a). Before day 22, Shannon diversity index increased under elevated pCO_2, whereas it is lowered under elevated pCO_2 level since day 24, although the differences were not statistically significant ($p = 0.161$, Fig. S8b).

4 Discussion

Ocean global changes have been suggested to alter community structure and reduce the phytoplankton diversity due to physicochemical environmental changes (Henson et al., 2021; Yuan et al., 2020). Specifically, there appears a growing trend of increasing dinoflagellates abundance relative to diatoms (Carreto et al., 2018). Our mesocosm experiment, conducted in the highly eutrophic Wuyuan Bay in the southern East China Sea during late autumn, also indicated that elevated pCO_2, along with the natural decrease of surface water temperature and declined nutrient availability, altered the structure and diversity of phytoplankton community. The diatom dominance corresponded to the decreased diversity and evenness of phytoplankton community, while these were recovered when the diatom dominance was replaced by dinoflagellates. However, this shift from diatoms to autotrophic dinoflagellates was relatively suppressed under elevated pCO_2 conditions. In our mesocosms, the dinoflagellates that emerged during the mid-phase (e.g., *Protoperidinium* sp., *Pentapharsodinium dalei* and *Heterocapsa* sp., Fig. S9a) were predominantly small (< 20 µm, Fig. S4g) (Gu et al., 2013; Hanifah et al., 2022), but these dinoflagellates were soon replaced by an even smaller size fraction, in-

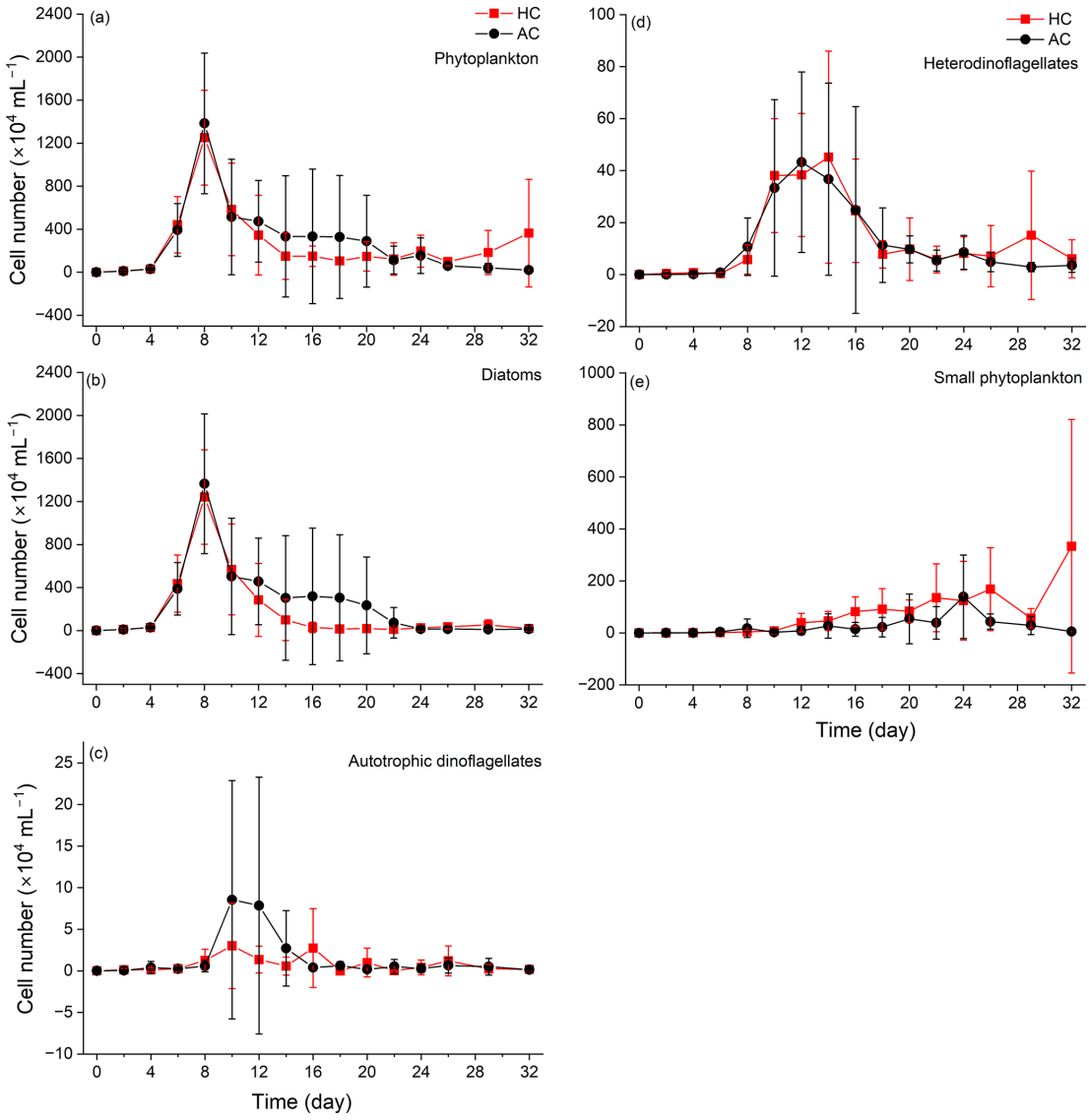

Figure 5. Temporal variations of phytoplankton **(a)**, diatoms **(b)**, autotrophic dinoflagellates **(c)**, heterodinoflagellates **(d)** and **(e)** small phytoplankton (Cyanobacteria, Chlorophyta, Cryptophyta and Euglenophyta) cell numbers in HC (1000 µatm) and AC (410 µatm) mesocosms. Data are means ± SD of 5 replicates for HC and 4 replicates for AC mesocosms.

cluding Cyanobacteria, Chlorophyta, Cryptophytes, and Euglenophyta (Figs. 5, 6, and S4). Ultimately, these smaller taxa maintained the primary production of phytoplankton communities after nutrient depletion (Fig. 4).

When diatoms dominated the phytoplankton community (before day 8), primary production per water volume and per Chl *a* did not change in the same pattern with increased diatom biomass (Fig. 4). This is likely attributable to the larger size of photosynthetic unit (PSU) and lower reaction center-to-Chl *a* ratio in diatoms, which could result in relatively lower photosynthetic efficiency (Wu et al., 2014; Malerba et al., 2018). Meanwhile, The competitive advantages conferred by CO_2-concentrating mechanisms (CCMs) in diatoms led to insignificant lower biomass (Figs. 5b and S7a) but higher primary production per water volume and per µg Chl *a* (Fig. 4a, b, d and e) under elevated pCO_2: their higher CO_2 affinity and CCMs plasticity may help diatoms gain a competitive advantage in DIC uptake under ocean acidification scenarios (Huang et al., 2021; Raven and Beardall, 2020). Furthermore, the down-regulated of CCMs in diatoms can save energy for other physiology processes and thereby fuel their primary production (see the review by Gao and Campbell, 2014 and the references therein). These benefits resulting from elevated pCO_2 also led to higher diversity and evenness (Fig. S8a and b), suggesting that more diatom species were benefited from the elevated pCO_2. While previous works have demonstrated a positive effect of elevated pCO_2 on the photosynthetic carbon fixation by di-

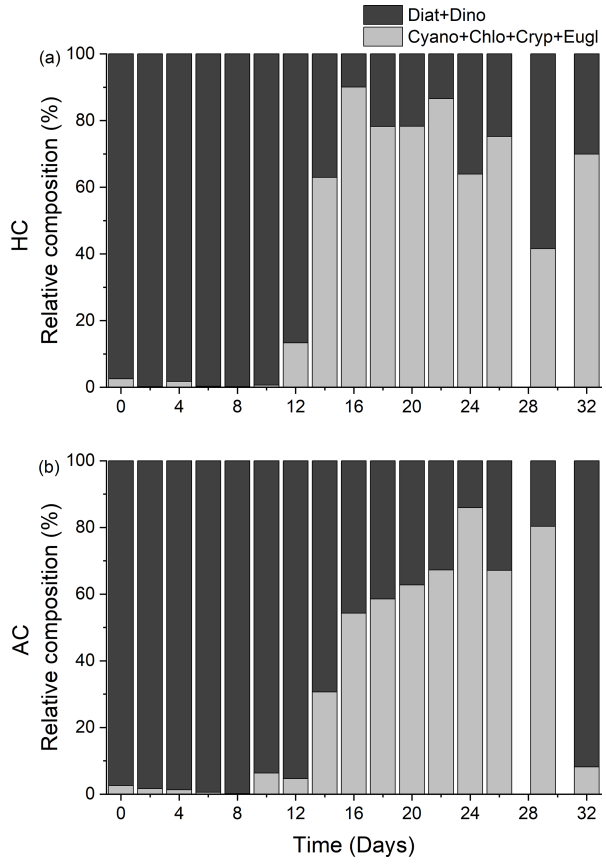

Figure 6. Temporal variations of the relative composition of diatoms + dinoflagellates (Diat + Dino, black), Cyanobacteria + Chlorophyta + Cryptophytes + Euglenophyta (Cyano + Chlo + Cryp + Eugl, grey) in HC (1000 µatm, **a**) and AC (410 µatm, **b**) mesocosms. Data are means of 5 replicates for HC and 4 replicates for AC mesocosms.

atoms grown under low light and phytoplankton assemblages in waters of higher nutrient availability (Gao et al., 2022), our results (Figs. 5b and S1) indicate that nutrient limitation can override or even reverse to the positive effects of elevated pCO_2 on diatoms (Boyd et al., 2016; Li et al., 2018).

It appeared that dinoflagellates were less sensitive to the depletion of nutrients compared to diatoms, with autotrophic dinoflagellates were more sensitive to elevated pCO_2 (Figs. 5c and S7b). These suppressed transition from diatoms to autotrophic dinoflagellates under the elevated pCO_2 was consistent with our previous works, though conducted in different seasons (Huang et al., 2021), which is likely due to the different CCMs efficiency and/or acidic resilience between dinoflagellates and diatoms. Since the affinity of ribulose 1, 5-diphosphate carboxylase/oxidase (Rubisco) for CO_2 is much lower in autotrophic dinoflagellates than in diatoms (Reinfelder, 2011), elevated pCO_2 must have benefitted the former more compared the latter, though invisible growth advantage was observed on the autotrophic dinoflagellates between days 8 and 16. The heterodinoflagellates can utilize organic matters (Glibert and Legrand, 2006) and prey on microbes including bacteria and smaller microalgae (Jeong et al., 2010). This versatile nutrition strategy supported their rapid bloom starting from day 8, leading to the replacement of autotrophic ones from day 12 onward (Fig. 5c and d). Although they were shown to be insensitive to ocean acidification (Meunier et al., 2017), their respiration was depressed due to the acidic stress, raising their resilience in terms of energetic cost (Wang and Gao, 2024). These mechanisms likely explain the observed insignificant effects of HC on heterodinoflagellates.

The gradual increase in SiO_3^{2-} concentration, a nutrient exclusively required by diatoms, coincided with their decline, confirming the low abundance of diatoms in the mid and late phase of experiment, while the slightly increases in $NO_3^- + NO_2^-$, PO_4^{3-} and SiO_3^{2-} concentrations from day 10 onward (Fig. 2a, e, and f) should be attributed to remineralization by heterotrophic bacteria (Arístegui et al., 2009; Bunse and Pinhassi, 2017). These regenerated $NO_3^- + NO_2^-$ and PO_4^{3-} subsequently refueled the growth of small phytoplankton taxa, recover the diversity and evenness in the phytoplankton communities (Figs. 5e and S8a, b) (Thingstad and Rassoulzadegan, 1995). Alternatively, it is plausible that grazing activity by zooplankton, which was not quantifited in this study, also contributed to the apparent rise in diversity and evenness, as grazers tend to consume dominant phytoplankton taxa (Thingstad and Rassoulzadegan, 1999; Calbet and Landry, 2004).

The dominant small taxa, such as *Cryptophyta* sp. and green microalga *Pyramimonas* sp. (Fig. S4h and i) during days 16–24, achieved primary productivity (per µg Chl *a*) comparable to the diatom-dominated community observed on days 4–6 (Fig. 4b and d). The success of these small taxa after nutrient depletion can be attributed to their small size and larger surface-to-volume ratio (Finkel et al., 2009; Giordano et al., 2005), which might enable them with higher efficiency in nutrients uptake and CO_2 diffusion. Furthermore, the higher abundance of viruses and heterotrophic bacteria in the HC mesocosms (Huang et al., 2021; Lin et al., 2018) intensified nutrient remineralization, subsidizing these small, fast-growing phototrophs and leading to their earlier emergence on day 16 compared to day 24 in the AC mesocosms (Fig. 6). While it's possible that picophytoplankton originally present in this region (Zhong et al., 2020) were missed by microscope-based identification, it is reasonable to infer that they also contributed to the late-phase primary production. Previous studies indicated that, after diatom/dinoflagella blooms and nutrient depletion, remineralized nutrients in the seawater may also favor the growth of picophytoplankton (Nishibe et al., 2015; Fu et al., 2009) and elevated pCO_2 would further benefit their growth. Thus, it is likely that, picophytoplankton also dominated the phytoplankton communities in the HC mesocosms.

Though previous studies have suggested the changing temperatures influenced the phytoplankton growth and community structure individually or interactively with OA and other environmental factors (Bénard et al., 2018; Courboulès et al., 2021; Li et al., 2018), the results from the present autumn mesocosm experiment revealed the same pattern with our previous spring mesocosm experiment (Huang et al., 2021), suggesting that it is not the seasonal temperature trajectories but the availability of nutrients that controlled the shift from diatom to dinoflagellate dominance, leading to declines in primary productivity (Huang et al., 2021; Cloern, 1996). Such consistency underscores that nutrient availability and stoichiometry are the primary determinants of phytoplankton community composition, usually exerting stronger and more immediate effects on taxonomic and functional group dominance (Karl et al., 1996; Paerl and Paul, 2012; Ptacnik et al., 2008; Meyer et al., 2016), though thermal and acidic stresses can impact phytoplankton photosynthesis and respiration to greater extent under nutrient limitation (Li et al., 2018; Gao et al., 2022).

Reduced nutrient availability usually decreases phytoplankton community richness (Gazeau et al., 2017), although ocean acidification appeared to partly offset such effects (Fig. S8). However, these compensatory effects diminished once both the initial and regenerated nitrogen sources were exhausted (after day 24, Fig. S8b). At that point, only a few small phytoplankton taxa tolerant to low pH remained dominant, indicating a loss of diversity in the community and less stable ecosystems (Mccann, 2000) under combination of acidic stress and nutrient limitation. In summary, beyond compensating previous works, our study further demonstrated that progressive ocean acidification is likely to reduce primary production and phytoplankton diversity in the eutrophicated coastal water of the southern East China Sea.

Data availability. All relevant data are presented in the paper and its Supplement, and will be available upon request to the corresponding author Kunshan Gao.

Supplement. The supplement related to this article is available online at https://doi.org/10.5194/bg-23-4515-2026-supplement.

Author contributions. Kunshan Gao and Guang Gao designed the mesocosm experiment; Yuming Rao, Na Wang, Jiazhen Sun, Xiaowen Jiang, Di Zhang, Liming Qu, He Li, Qianqian Fu, Xuyang Wang, Cong Zhou, Zichao Deng, Yang Tian, Xiangqi Yi, Ruiping Huang performed the mesocosm experiment. Yuming Rao analyzed the data and wrote up the manuscript. Na Wang performed microscopy observation; Kunshan Gao edited the manuscript. All authors reviewed and contributed to revision of the manuscript.

Competing interests. The contact author has declared that none of the authors has any competing interests.

Disclaimer. Publisher's note: Copernicus Publications remains neutral with regard to jurisdictional claims made in the text, published maps, institutional affiliations, or any other geographical representation in this paper. The authors bear the ultimate responsibility for providing appropriate place names. Views expressed in the text are those of the authors and do not necessarily reflect the views of the publisher.

Acknowledgements. We are grateful to the engineers, Xianglan Zeng and Wenyan Zhao, for their technical supports, and we thank Prof. Jian Ma (College of the Environment and Ecology, Xiamen University) for providing the Environmental Water Analyzer (iSEA) during the mesocosm experiment.

Financial support. This research has been supported by the National Key Research and Development Program of China (grant no. 2022YFC3105303) and the National Natural Science Foundation of China (grant nos. 42361144840 and 41720104005).

Review statement. This paper was edited by Stefano Ciavatta and reviewed by two anonymous referees.

References

Arístegui, J., Gasol, J. M., Duarte, C. M., and Herndld, G. J.: Microbial oceanography of the dark ocean's pelagic realm, Limnol. Oceanogr., 54, 1501–1529, https://doi.org/10.4319/lo.2009.54.5.1501, 2009.

Bach, L. T., Taucher, J., Boxhammer, T., Ludwig, A., The Kristineberg, K. C., Achterberg, E. P., Algueró-Muñiz, M., Anderson, L. G., Bellworthy, J., Büdenbender, J., Czerny, J., Ericson, Y., Esposito, M., Fischer, M., Haunost, M., Hellemann, D., Horn, H. G., Hornick, T., Meyer, J., Sswat, M., Zark, M., and Riebesell, U.: Influence of Ocean Acidification on a Natural Winter-to-Summer Plankton Succession: First Insights from a Long-Term Mesocosm Study Draw Attention to Periods of Low Nutrient Concentrations, PLOS ONE, 11, e0159068, https://doi.org/10.1371/journal.pone.0159068, 2016.

Bach, L. T., Hernández-Hernández, N., Taucher, J., Spisla, C., Sforna, C., Riebesell, U., and Arístegui, J.: Effects of Elevated CO_2 on a Natural Diatom Community in the Subtropical NE Atlantic, Front. Mar. Sci., 6, https://doi.org/10.3389/fmars.2019.00075, 2019.

Bénard, R., Levasseur, M., Scarratt, M., Blais, M.-A., Mucci, A., Ferreyra, G., Starr, M., Gosselin, M., Tremblay, J.-É., and Lizotte, M.: Experimental assessment of the sensitivity of an estuarine phytoplankton fall bloom to acidification and warming, Biogeosciences, 15, 4883–4904, https://doi.org/10.5194/bg-15-4883-2018, 2018.

Boyd, P. W., Dillingham, P. W., McGraw, C. M., Armstrong, E. A., Cornwall, C. E., Feng, Y. Y., Hurd, C. L., Gault-Ringold, M., Roleda, M. Y., Timmins-Schiffman, E., and Nunn, B. L.: Physiological responses of a Southern Ocean diatom to complex future ocean conditions, Nat. Clim. Change., 6, 207–213, https://doi.org/10.1038/nclimate2811, 2016.

Bunse, C. and Pinhassi, J.: Marine Bacterioplankton Seasonal Succession Dynamics, Trends Microbiol., 25, 494–505, https://doi.org/10.1016/j.tim.2016.12.013, 2017.

Cai, W.-J., Hu, X., Huang, W.-J., Murrell, M. C., Lehrter, J. C., Lohrenz, S. E., Chou, W.-C., Zhai, W., Hollibaugh, J. T., and Wang, Y.: Acidification of subsurface coastal waters enhanced by eutrophication, Nat. Geosci., 4, 766–770, 2011.

Calbet, A. and Landry, M. R.: Phytoplankton growth, microzooplankton grazing, and carbon cycling in marine systems, Limnol. Oceanogr., 49, 51–57, https://doi.org/10.4319/lo.2004.49.1.0051, 2004.

Canadell, J. G., Monteiro, P. M., Costa, M. H., Cotrim da Cunha, L., Cox, P. M., Eliseev, A. V., Henson, S., Ishii, M., Jaccard, S., and Koven, C.: Intergovernmental Panel on Climate Change (IPCC). Global carbon and other biogeochemical cycles and feedbacks, in: Climate change 2021: The physical science basis. Contribution of working group I to the sixth assessment report of the intergovernmental panel on climate change, Cambridge University Press, 673–816, https://doi.org/10.1017/9781009157896.007, 2023.

Carreto, J. I., Carignan, M. O., Montoya, N. G., Cozzolino, E., and Akselman, R.: Mycosporine-like amino acids and xanthophyll-cycle pigments favour a massive spring bloom development of the dinoflagellate Prorocentrum minimum in Grande Bay (Argentina), an ozone hole affected area, J. Marine Syst., 178, 15–28, https://doi.org/10.1016/j.jmarsys.2017.10.004, 2018.

Chauhan, N., Dedman, C. J., Baldreki, C., Dowle, A. A., Larson, T. R., and Rickaby, R. E. M.: Contrasting species-specific stress response to environmental pH determines the fate of coccolithophores in future oceans, Mar. Pollut. Bull., 209, 117136, https://doi.org/10.1016/j.marpolbul.2024.117136, 2024.

Cloern, J. E.: Phytoplankton bloom dynamics in coastal ecosystems: A review with some general lessons from sustained investigation of San Francisco Bay, California, Rev. Geophys., 34, 127–168, https://doi.org/10.1029/96RG00986, 1996.

Courboulès, J., Vidussi, F., Soulié, T., Mas, S., Pecqueur, D., and Mostajir, B.: Effects of experimental warming on small phytoplankton, bacteria and viruses in autumn in the Mediterranean coastal Thau Lagoon, Aquat. Ecol., 55, 647–666, https://doi.org/10.1007/s10452-021-09852-7, 2021.

Dai, M., Wang, L., Guo, X., Zhai, W., Li, Q., He, B., and Kao, S.-J.: Nitrification and inorganic nitrogen distribution in a large perturbed river/estuarine system: the Pearl River Estuary, China, Biogeosciences, 5, 1227–1244, https://doi.org/10.5194/bg-5-1227-2008, 2008.

Engel, A., Zondervan, I., Aerts, K., Beaufort, L., Benthien, A., Chou, L., Delille, B., Gattuso, J.-P., Harlay, J., and Heemann, C.: Testing the direct effect of CO_2 concentration on a bloom of the coccolithophorid *Emiliania huxleyi* in mesocosm experiments, Limnol. Oceanogr., 50, 493–507, 2005.

Feng, Y., Xiong, Y., Hall-Spencer, J. M., Liu, K., Beardall, J., Gao, K., Ge, J., Xu, J., and Gao, G.: Shift in algal blooms from micro- to macroalgae around China with increasing eutrophication and climate change, Glob. Change Biol., 30, e17018, https://doi.org/10.1111/gcb.17018, 2024.

Finkel, Z. V., Beardall, J., Flynn, K. J., Quigg, A., Rees, T. A. V., and Raven, J. A.: Phytoplankton in a changing world: cell size and elemental stoichiometry, J. Plankton. Res., 32, 119–137, https://doi.org/10.1093/plankt/fbp098, 2009.

Friedlingstein, P., O'Sullivan, M., Jones, M. W., Andrew, R. M., Hauck, J., Landschützer, P., Le Quéré, C., Li, H., Luijkx, I. T., Olsen, A., Peters, G. P., Peters, W., Pongratz, J., Schwingshackl, C., Sitch, S., Canadell, J. G., Ciais, P., Jackson, R. B., Alin, S. R., Arneth, A., Arora, V., Bates, N. R., Becker, M., Bellouin, N., Berghoff, C. F., Bittig, H. C., Bopp, L., Cadule, P., Campbell, K., Chamberlain, M. A., Chandra, N., Chevallier, F., Chini, L. P., Colligan, T., Decayeux, J., Djeutchouang, L. M., Dou, X., Duran Rojas, C., Enyo, K., Evans, W., Fay, A. R., Feely, R. A., Ford, D. J., Foster, A., Gasser, T., Gehlen, M., Gkritzalis, T., Grassi, G., Gregor, L., Gruber, N., Gürses, Ö., Harris, I., Hefner, M., Heinke, J., Hurtt, G. C., Iida, Y., Ilyina, T., Jacobson, A. R., Jain, A. K., Jarníková, T., Jersild, A., Jiang, F., Jin, Z., Kato, E., Keeling, R. F., Klein Goldewijk, K., Knauer, J., Korsbakken, J. I., Lan, X., Lauvset, S. K., Lefèvre, N., Liu, Z., Liu, J., Ma, L., Maksyutov, S., Marland, G., Mayot, N., McGuire, P. C., Metzl, N., Monacci, N. M., Morgan, E. J., Nakaoka, S.-I., Neill, C., Niwa, Y., Nützel, T., Olivier, L., Ono, T., Palmer, P. I., Pierrot, D., Qin, Z., Resplandy, L., Roobaert, A., Rosan, T. M., Rödenbeck, C., Schwinger, J., Smallman, T. L., Smith, S. M., Sospedra-Alfonso, R., Steinhoff, T., Sun, Q., Sutton, A. J., Séférian, R., Takao, S., Tatebe, H., Tian, H., Tilbrook, B., Torres, O., Tourigny, E., Tsujino, H., Tubiello, F., van der Werf, G., Wanninkhof, R., Wang, X., Yang, D., Yang, X., Yu, Z., Yuan, W., Yue, X., Zaehle, S., Zeng, N., and Zeng, J.: Global Carbon Budget 2024, Earth Syst. Sci. Data, 17, 965–1039, https://doi.org/10.5194/essd-17-965-2025, 2025.

Fu, M., Wang, Z., Li, Y., Li, R., Sun, P., Wei, X., Lin, X., and Guo, J.: Phytoplankton biomass size structure and its regulation in the Southern Yellow Sea (China): Seasonal variability, Cont. Shelf. Res., 29, 2178–2194, https://doi.org/10.1016/j.csr.2009.08.010, 2009.

Gao, K.: Approaches and involved principles to control pH/pCO_2 stability in algal cultures, J. Appl. Phycol, 33, 3497–3505, 2021.

Gao, K. and Campbell, D. A.: Photophysiological responses of marine diatoms to elevated CO_2 and decreased pH: a review, Funct. Plant Biol., 41, 449–459, https://doi.org/10.1071/FP13247, 2014.

Gao, K., Xu, J., Gao, G., Li, Y., Hutchins, D. A., Huang, B., Wang, L., Zheng, Y., Jin, P., and Cai, X.: Rising CO_2 and increased light exposure synergistically reduce marine primary productivity, Nat. Clim. Change, 2, 519–523, 2012.

Gao, K., Gao, G., Wang, Y., and Dupont, S.: Impacts of ocean acidification under multiple stressors on typical organisms and ecological processes, Mar. Life Sci. Tech., 2, 279–291, 2020.

Gao, K., Zhao, W., and Beardall, J.: Future Responses of Marine Primary Producers to Environmental Changes, in: Blue Planet, Red and Green Photosynthesis, edited by: Maberly, S. C. and Gontero, B., 273–304, https://doi.org/10.1002/9781119986782.ch9, 2022.

Gattuso, J.-P., Magnan, A., Billé, R., Cheung, W. W., Howes, E. L., Joos, F., Allemand, D., Bopp, L., Cooley, S. R., and Eakin, C. M.: Contrasting futures for ocean and society from different

anthropogenic CO_2 emissions scenarios, Science, 349, aac4722, https://doi.org/10.1126/science.aac4722, 2015.

Gazeau, F., Sallon, A., Pitta, P., Tsiola, A., Maugendre, L., Giani, M., Celussi, M., Pedrotti, M. L., Marro, S., and Guieu, C.: Limited impact of ocean acidification on phytoplankton community structure and carbon export in an oligotrophic environment: Results from two short-term mesocosm studies in the Mediterranean Sea, Estuar. Coast. Shelf. S., 186, 72–88, https://doi.org/10.1016/j.ecss.2016.11.016, 2017.

Giordano, M., Norici, A., and Hell, R.: Sulfur and phytoplankton: acquisition, metabolism and impact on the environment, New. Phytol., 166, 371–382, 2005.

Glibert, P. M. and Legrand, C.: The Diverse Nutrient Strategies of Harmful Algae: Focus on Osmotrophy, in: Ecology of Harmful Algae, edited by: Granéli, E. and Turner, J. T., Springer Berlin Heidelberg, Berlin, Heidelberg, 163–175, https://doi.org/10.1007/978-3-540-32210-8_13, 2006.

Gu, H., Luo, Z., Zeng, N., Lan, B., and Lan, D.: First record of *Pentapharsodinium* (Peridiniales, Dinophyceae) in the China Sea, with description of *Pentapharsodinium dalei* var. aciculiferum, Phycol. Res., 61, 256–267, https://doi.org/10.1111/pre.12024, 2013.

Hanifah, A. H., Teng, S. T., Law, I. K., Abdullah, N., Chiba, S. U. A., Lum, W. M., Tillmann, U., Lim, P. T., and Leaw, C. P.: Six marine thecate *Heterocapsa* (Dinophyceae) from Malaysia, including the description of three novel species and their cytotoxicity potential, Harmful Algae, 120, 102338, https://doi.org/10.1016/j.hal.2022.102338, 2022.

Hasle, G. R. and Syvertsen, E. E.: Chapter 2 – Marine Diatoms, in: Identifying Marine Phytoplankton, edited by: Tomas, C. R., Academic Press, San Diego, 5–385, https://doi.org/10.1016/B978-012693018-4/50004-5, 1997.

Henson, S. A., Cael, B. B., Allen, S. R., and Dutkiewicz, S.: Future phytoplankton diversity in a changing climate, Nat. Commun., 12, 5372, https://doi.org/10.1038/s41467-021-25699-w, 2021.

Huang, R., Sun, J., Yang, Y., Jiang, X., Wang, Z., Song, X., Wang, T., Zhang, D., Li, H., and Yi, X.: Elevated pCO_2 Impedes Succession of Phytoplankton Community From Diatoms to Dinoflagellates Along With Increased Abundance of Viruses and Bacteria, Front. Mar. Sci, 8, 642208, https://doi.org/10.3389/fmars.2021.642208, 2021.

Jeong, H. J., Yoo, Y. D., Kim, J. S., Seong, K. A., Kang, N. S., and Kim, T. H.: Growth, feeding and ecological roles of the mixotrophic and heterotrophic dinoflagellates in marine planktonic food webs, Ocean. Sci. J., 45, 65–91, https://doi.org/10.1007/s12601-010-0007-2, 2010.

Karl, D. M., Christian, J. R., Dore, J. E., Hebel, D. V., Letelier, R. M., Tupas, L. M., and Winn, C. D.: Seasonal and interannual variability in primary production and particle flux at Station ALOHA, Deep-Sea. Res. Pt. II, 43, 539–568, https://doi.org/10.1016/0967-0645(96)00002-1, 1996.

Intergovernmental Oceanographic Commission: Protocols for the Joint Global Ocean Flux Study (JGOFS) Core Measurements, Paris, France, UNESCO-IOC, 170 pp., Intergovernmental Oceanographic Commission Manuals and Guides: 29, JGOFS Report; 19, https://doi.org/10.25607/OBP-1409, 1994.

Li, F., Beardall, J., and Gao, K.: Diatom performance in a future ocean: interactions between nitrogen limitation, temperature, and CO_2-induced seawater acidification, ICES J. Mar. Sci., 75, 1451–1464, https://doi.org/10.1093/icesjms/fsx239, 2018.

Li, Q., Wang, F., Wang, Z. A., Yuan, D., Dai, M., Chen, J., Dai, J., and Hoering, K. A.: Automated Spectrophotometric Analyzer for Rapid Single-Point Titration of Seawater Total Alkalinity, Environ. Sci. Technol., 47, 11139–11146, https://doi.org/10.1021/es402421a, 2013.

Lin, X., Huang, R., Li, Y., Li, F., Wu, Y., Hutchins, D. A., Dai, M., and Gao, K.: Interactive network configuration maintains bacterioplankton community structure under elevated CO_2 in a eutrophic coastal mesocosm experiment, Biogeosciences, 15, 551–565, https://doi.org/10.5194/bg-15-551-2018, 2018.

Liu, N., Tong, S., Yi, X., Li, Y., Li, Z., Miao, H., Wang, T., Li, F., Yan, D., Huang, R., Wu, Y., Hutchins, D. A., Beardall, J., Dai, M., and Gao, K.: Carbon assimilation and losses during an ocean acidification mesocosm experiment, with special reference to algal blooms, Mar. Environ. Res., 129, 229–235, https://doi.org/10.1016/j.marenvres.2017.05.003, 2017.

Ma, J., Li, P., Chen, Z., Lin, K., Chen, N., Jiang, Y., Chen, J., Huang, B., and Yuan, D.: Development of an Integrated Syringe-Pump-Based Environmental-Water Analyzer (iSEA) and Application of It for Fully Automated Real-Time Determination of Ammonium in Fresh Water, Anal. Chem., 90, 6431–6435, https://doi.org/10.1021/acs.analchem.8b01490, 2018.

Malerba, M. E., Palacios, M. M., Palacios Delgado, Y. M., Beardall, J., and Marshall, D. J.: Cell size, photosynthesis and the package effect: an artificial selection approach, New. Phytol., 219, 449–461, https://doi.org/10.1111/nph.15163, 2018.

McCann, K. S.: The diversity–stability debate, Nature, 405, 228–233, https://doi.org/10.1038/35012234, 2000.

Meakin, N. G. and Wyman, M.: Rapid shifts in picoeukaryote community structure in response to ocean acidification, ISME J., 5, 1397–1405, https://doi.org/10.1038/ismej.2011.18, 2011.

Meunier, C. L., Algueró-Muñiz, M., Horn, H. G., Lange, J. A. F., and Boersma, M.: Direct and indirect effects of near-future CO_2 levels on zooplankton dynamics, Mar. Freshwater. Res., 68, 373–380, https://doi.org/10.1071/MF15296, 2017.

Meyer, J., Löscher, C. R., Neulinger, S. C., Reichel, A. F., Loginova, A., Borchard, C., Schmitz, R. A., Hauss, H., Kiko, R., and Riebesell, U.: Changing nutrient stoichiometry affects phytoplankton production, DOP accumulation and dinitrogen fixation – a mesocosm experiment in the eastern tropical North Atlantic, Biogeosciences, 13, 781–794, https://doi.org/10.5194/bg-13-781-2016, 2016.

Nishibe, Y., Takahashi, K., Shiozaki, T., Kakehi, S., Saito, H., and Furuya, K.: Size-fractionated primary production in the Kuroshio Extension and adjacent regions in spring, J. Oceanogr., 71, 27–40, https://doi.org/10.1007/s10872-014-0258-0, 2015.

Paerl, H. W. and Paul, V. J.: Climate change: Links to global expansion of harmful cyanobacteria, Water. Res., 46, 1349–1363, https://doi.org/10.1016/j.watres.2011.08.002, 2012.

Paul, A. J. and Bach, L. T.: Universal response pattern of phytoplankton growth rates to increasing CO_2, New. Phytol., 228, 1710–1716, https://doi.org/10.1111/nph.16806, 2020.

Ptacnik, R., Solimini, A. G., Andersen, T., Tamminen, T., Brettum, P., Lepistö, L., Willén, E., and Rekolainen, S.: Diversity predicts stability and resource use efficiency in natural phytoplankton communities, P. Natl. Acad. Sci. USA, 105, 5134–5138, https://doi.org/10.1073/pnas.0708328105, 2008.

Raven, J. A. and Beardall, J.: Energizing the plasmalemma of marine photosynthetic organisms: the role of primary active transport, J. Mar. Biol. Assoc. UK, 100, 333–346, 2020.

Reinfelder, J. R.: Carbon concentrating mechanisms in eukaryotic marine phytoplankton, Annu. Rev. Mar. Sci, 3, 291–315, 2011.

Riebesell, U., Bach, L. T., Bellerby, R. G., Monsalve, J. R. B., Boxhammer, T., Czerny, J., Larsen, A., Ludwig, A., and Schulz, K. G.: Competitive fitness of a predominant pelagic calcifier impaired by ocean acidification, Nat. Geosci., 10, 19–23, 2017.

Ritchie, R. J.: Consistent sets of spectrophotometric chlorophyll equations for acetone, methanol and ethanol solvents, Photosynth. Res., 89, 27–41, 2006.

Rogelj, J., Shindell, D., Jiang, K., Fifita, S., Forster, P., Ginzburg, V.,, Handa, C., Kheshgi, H., Kobayashi, S., Kriegler, E., Mundaca,, and L., S., R., and Vilariño, M. V.: Mitigation Pathways Compatible with 1.5 °C in the Context of Sustainable Development, in: Global Warming of 1.5 °C: IPCC Special Report on Impacts of Global Warming of 1.5 °C above Pre-industrial Levels in Context of Strengthening Response to Climate Change, Sustainable Development, and Efforts to Eradicate Poverty, edited by: Intergovernmental Panel on Climate Change, Cambridge University Press, Cambridge, 93–174, https://doi.org/10.1017/9781009157940.004, 2022.

Rokitta, S. D., John, U., and Rost, B.: Ocean acidification affects redox-balance and ion-homeostasis in the life-cycle stages of *Emiliania huxleyi*, Plos One, 7, e52212, https://doi.org/10.1371/journal.pone.0052212, 2012.

Schulz, K. G., Bellerby, R. G. J., Brussaard, C. P. D., Büdenbender, J., Czerny, J., Engel, A., Fischer, M., Koch-Klavsen, S., Krug, S. A., Lischka, S., Ludwig, A., Meyerhöfer, M., Nondal, G., Silyakova, A., Stuhr, A., and Riebesell, U.: Temporal biomass dynamics of an Arctic plankton bloom in response to increasing levels of atmospheric carbon dioxide, Biogeosciences, 10, 161–180, https://doi.org/10.5194/bg-10-161-2013, 2013.

State Oceanic Administration: Technical specification for red tide monitoring (In Chinese), HY/T 069-2005, https://std.samr.gov.cn/hb/search/stdHBDetailed?id=8B1827F1ACF7BB19E05397BE0A0AB44A (last access: 29 June 2026), 2005.

Steidinger, K. A. and Jangen, K.: Chapter 3 – Dinoflagellates, in: Identifying Marine Phytoplankton, edited by: Tomas, C. R., Academic Press, San Diego, 387–584, https://doi.org/10.1016/B978-012693018-4/50005-7, 1997.

Stukel, M. R., Irving, J. P., Kelly, T. B., Ohman, M. D., Fender, C. K., and Yingling, N.: Carbon sequestration by multiple biological pump pathways in a coastal upwelling biome, Nat. Commun., 14, 2024, https://doi.org/10.1038/s41467-023-37771-8, 2023.

Tanaka, T., Alliouane, S., Bellerby, R. G. B., Czerny, J., de Kluijver, A., Riebesell, U., Schulz, K. G., Silyakova, A., and Gattuso, J.-P.: Effect of increased pCO_2 on the planktonic metabolic balance during a mesocosm experiment in an Arctic fjord, Biogeosciences, 10, 315–325, https://doi.org/10.5194/bg-10-315-2013, 2013.

Taylor, A. R., Brownlee, C., and Wheeler, G.: Coccolithophore cell biology: chalking up progress, Annu. Rev. Mar. Sci, 9, 283–310, 2017.

Thingstad, T. F. and Rassoulzadegan, F.: Nutrient limitations, microbial food webs and 'biological C-pumps': suggested interactions in a P-limited Mediterranean, Mar. Ecol. Prog. Ser., 117, 299–306, 1995.

Thingstad, T. F. and Rassoulzadegan, F.: Conceptual models for the biogeochemical role of the photic zone microbial food web, with particular reference to the Mediterranean Sea, Prog. Oceanogr., 44, 271–286, https://doi.org/10.1016/S0079-6611(99)00029-4, 1999.

Vázquez, V., León, P., Gordillo, F. J. L., Jiménez, C., Concepción, I., Mackenzie, K., Bresnan, E., and Segovia, M.: High-CO_2 Levels Rather than Acidification Restrict *Emiliania huxleyi* Growth and Performance, Microb. Ecol., 86, 127–143, https://doi.org/10.1007/s00248-022-02035-3, 2023.

Wang, N. and Gao, K.: Ocean acidification and food availability impacts on the metabolism and grazing in a cosmopolitan herbivorous protist Oxyrrhis marina, Front. Mar. Sci, 11, https://doi.org/10.3389/fmars.2024.1371296, 2024.

Wu, Y., Jeans, J., Suggett, D. J., Finkel, Z. V., and Campbell, D. A.: Large centric diatoms allocate more cellular nitrogen to photosynthesis to counter slower RUBISCO turnover rates, Front. Mar. Sci, 1, 2014, https://doi.org/10.3389/fmars.2014.00068, 2014.

Wu, Y., Campbell, D. A., and Gao, K.: Short-term elevated CO_2 exposure stimulated photochemical performance of a coastal marine diatom, Mar. Environ. Res., 125, 42–48, https://doi.org/10.1016/j.marenvres.2016.12.001, 2017.

Yang, S. and Liu, X.: Characteristics of phytoplankton assemblages in the southern Yellow Sea, China, Mar. Pollut. Bull., 135, 562–568, 2018.

Yuan, Z., Liu, D., Masqué, P., Zhao, M., Song, X., and Keesing, J. K.: Phytoplankton Responses to Climate-Induced Warming and Interdecadal Oscillation in North-Western Australia, Paleoceanogr. Paleocl., 35, e2019PA003712, https://doi.org/10.1029/2019PA003712, 2020.

Zhong, Y., Liu, X., Xiao, W., Laws, E. A., Chen, J., Wang, L., Liu, S., Zhang, F., and Huang, B.: Phytoplankton community patterns in the Taiwan Strait match the characteristics of their realized niches, Prog. Oceanogr., 186, 102366, https://doi.org/10.1016/j.pocean.2020.102366, 2020.